# β-diketone functionalized SBA-15 and SBA-16 for rapid liquid–solid extraction of copper

## R. Ouargli, R. Hamacha, N. Benharrats, A. Boos & A. Bengueddach

MICROPOROUS–ZSM 5          6 nm

MESOPOROUS–MCM 41          10 nm

MACROPOROUS–APATITE          100.0 μm

Springer

Springer

Springer

# β-diketone functionalized SBA-15 and SBA-16 for rapid liquid–solid extraction of copper

R. Ouargli · R. Hamacha · N. Benharrats ·
A. Boos · A. Bengueddach

**Abstract** β-diketone functionalized SBA mesoporous materials were used successfully for the removal of copper from aqueous solution. SBA-15 and SBA-16 were impregnated with an acid ligand, 1-phenyl-3-methyl-4-stearoyl-5-pyrazolone (HPMSP) via the wet impregnation method. Characterization techniques showed that the highly ordered structure of the functionalized SBA is well retained after impregnation by the HPMSP. The effect of different extraction parameters, such as equilibrium time, extraction rate as a function of pH, nature of the medium (presence of $NO_3^-$ or $SO_4^{2-}$) and the extraction capacity has been studied and discussed. A copper uptake close to 99.99 % for functionalized SBA-15 and SBA-16 was achieved within only 5 min at lower pH values, thus the extraction kinetics are very rapid and instantaneous as attested by the immediate green coloration of the materials when mixed with copper solution. The extraction capacities of copper were determined about 22 and 25 mg/g at pH 3 respectively for SBA-15 CI and SBA-16 CI and fits well to the Langmuir isotherm equation.

**Keywords** Impregnation · HPMSP · Adsorption · Removal · Copper

R. Ouargli (✉) · R. Hamacha · A. Bengueddach
Laboratory of Materials Chemistry, Oran University, El M'naouer, BP 1524 , Oran, Algeria
e-mail: amiracl2000@yahoo.fr

R. Ouargli · N. Benharrats
Department of Materials Engineering, University of Science and Technology,  El M'naouer, BP 1505, Oran, Algeria

A. Boos
Institut pluridisciplinaire Hubert-Curien (IPHC), UMR 7178 CNRS, Strasbourg University, 25, rue Becquerel, 67087 Strasbourg Cedex 2, France

## 1 Introduction

The impact of the industrial waste on the environment became a serious ecological problem which worries the scientific and ecological community. These wastes produced by plastics, chemicals, paintings, metallurgy and nuclear industries contain generally heavy metals like Zn, Cu, Pb, Ni, Hg,… etc. [1]. These metals can be found by the way of leaching or other ways in sea waters, groundwater and wastewater. Such metals contaminated water which become toxic for human body and poses a severe threat to public health [2]. $Cu^{2+}$ ions are essential nutrients, but when people are exposed to copper levels above 1.3 mg/L for even short periods of time, stomach and intestinal problems occur. Longer exposure leads to kidney and liver damage [3, 4], and causes lung cancer and neurological diseases [5–7]. The production of DNA mutation is evidence of its carcinogenicity [8]. Within the strategy of fight against this pollution, the recovery of heavy metals is one of the principal solutions for industrial processing waste. Copper is recognized as one of the most harmful pollutants in the environment due to its high toxicity, non-degradability and bioaccumulation [9]. Thus, the rapid and effective removal of $Cu^{2+}$ from wastewater is among the most important issues in wastewater treatment. Various methods are used such as chemical precipitation [10], nanofiltration, ionic exchange [11], opposite osmosis [12] and solvent extraction. This last method presents some disadvantages such as the use of organic solvents, however these last years, the removal of heavy metals using functionalized solid supports like resins, clays and zeolites was largely studied by the scientific community [13–16], for example, MCM-41 impregnated by 3-phenyl-4-benzoyl-5-isoxazolone (HPBI) was tested successfully in the extraction of copper [17]. Compared to MCM-41, the more uniform pore structure and thicker silica walls of SBA-15 (31–64 Å)

are shown to impart significant stability to the material under hydrothermal conditions as well as an easier functionalization and application [18–21]. The SBA (Santa Barbara Amorphous) family was first synthesized in 1998 by using cationic surfactants [22] or non- ionic ones [18, 23]. This mesoporous material provides a lot of possibilities for the design and synthesis of open pore structures because of its high surface area and its easy controllable uniform pore size that may be extended to 300 Å. SBA-15 and SBA-16 with bi-dimensional hexagonal (P6mm) and tri-dimensional cubic (Im3m) respectively attracted a particular interest [24]. SBA-15 synthesized by using a triblock copolymer Pluronic P123 ($PEO_{20}PP0_{70}PE_{20}$) has the same structure as SBA-3 synthesized by cetyltrimethyl ammonium bromide [23], but with a larger pore diameter (>5 nm) and micropores in the silicate walls [24]. SBA-16 has inter-connected cavities in three dimensions [25] and is also synthesized under strongly acid conditions [18, 26, 27]. The studies concerning the recovery of copper using SBA, especially SBA-16 are rare [28, 29]. In the present work, a novel effective β-diketone functionalized SBA-15 CI and SBA-16 CI are proposed for the removal of copper (II). The mesoporous materials SBA-15 and SBA-16 are synthesized, calcined and impregnated with 1-phenyl-3-methyl-4-stearoyl-5-pyrazolone HPMSP (Fig. 1) via a wet process.

We systematically and deeply investigated the process of the extraction of the Cu(II) ions extraction; thus the influence of various experimental parameters, such as equilibrium time, solution pH, nature of the medium (presence of $NO_3^-$ or $SO_4^{2-}$) are studied. The initial metal ion concentration was also modified to determinate the extraction capacity of mesoporous SBA-15 CI and SBA-16 CI.

## 2 Experimental

### 2.1 Reagents

Pluronic P123 and Pluronic F127 (triblock organic copolymers, Aldrich) tetraethylorthosilicate (TEOS, 98 %, Aldrich), hydrochloric acid (HCl, 37 %, Fluka) and pure water MILLIQ were used for the synthesis of mesoporous materials. For the acid extractant HPMSP synthesis, we used 3-methyl-1-phenyl-2-pyrazoline-5-one ($H_2PMP$, Aldrich), calcium hydroxide ($Ca(OH)_2$, Sigma Aldrich), dioxane (Prolabop.a) and toluene/
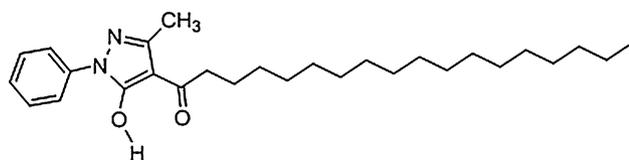


**Fig. 1** Molecular structure of HPMSP

ethanol (Aesar Alpha). Finally, chloroform (Sigma Aldrich) is used as solvent for the impregnation.

### 2.2 Synthesis of SBA-15, SBA-16 and HPMSP

SBA-15 C was prepared according to the procedure in the literature [18]: 6 g of P123 ($EO_{20}$–$PO_{70}$–$EO_{20}$) were stirred at 27 °C in 45 g of water and 180 g of 2 M HCl solution until total dissolution. Subsequently, 12.5 g of TEOS was added and the mixture was stirred at 37 °C for 20 h. The mixture was aged at 100 °C for 48 h. The white product was recovered through filtration, washed with pure water and dried at 60 °C overnight. Calcination was performed in oven at 550 °C for 6 h in air atmosphere in order to remove the triblock copolymer organic component with a heating rate of 1 °C/min.

SBA-16 C was synthesized according to the procedure in the literature [30]. In a typical synthesis: 0.47 g of P123 ($EO_{20}$–$PO_{70}$–$EO_{20}$) and 2.33 g of F127 ($EO_{106}$–$PO_{70}$–$EO_{106}$) were dissolved in a mixture of 24 g of $H_2O$ and 113 g of HCl (2 M) were added under stirring at 27 °C for 1 h. 10.4 g of TEOS was added under stirring for 20 h at 37 °C. The resultant hydrogel was placed in an autoclave and hated at 100 °C for 48 h. Finally, the product was filtered, washed with pure water and dried at 60 °C to obtain the sample as-synthesized (SBA-16 NC). Calcination was performed in oven at 550 °C for 6 h in air atmosphere.

The organic extractant 1-phenyl-3-methyl-4-stearoyl-5-pyrozolone (HPMSP) was prepared according to the method described by Jensen [31]. HPMSP was recrystallized several times in a toluene/ethanol mixture. Its color goes from brown to pale pink and purified by acid–base titration in a liquid biphasic system, TLC and $^1H$ NMR (300 Ultrashield, Bruker).

### 2.3 β-diketone functionalized mesoporous

The β-diketone functionalized mesoporous SBA-15 CI and SBA-16 CI are prepared by wet process. HPMSP and SBA-15 C (calcined) or SBA-16 C (calcined) are mixed with a mass ratio of 30 % in an adequate amount of chloroform under magnetic stirring during 6 h. The solvent is evaporated by using a rotavapor. The resultant products are dried at 40 °C overnight. After characterization, SBA-15 CI and SBA-16 CI are used in copper extraction.

### 2.4 Characterization of synthesized and functionalized mesoporous materials

The synthesized and functionalized SBA-15 C, SBA-16 C, SBA-15 CI and SBA-16 CI are characterized by FTIR ATR (Perkin Elmer, Spectrum One), nitrogen adsorption and desorption isotherms (SORPTOMATIC 1990, ThermoQuest), UV (HP 8453, Hewlett Packard) and SAXS

measurements. X-ray diagrams were obtained in transmission in the 300–20 Å window, with a homemade instrument by using a focused CuK$\alpha$1 linear beam, temperature control being within 0.03 °C on powder samples placed in sealed cells. The acquisition was performed on imaging plates, patterns being integrated to linear profiles.

## 2.5 Extraction experiments

In order to determine the influence of contact time, pH, presence of counter-ions and extraction capacity of SBA-15 CI and SBA-16 CI for $Cu^{2+}$ adsorption, 100 mg of SBA-15 CI or SBA-16 CI are shaken within 10 mL of a $Cu^{2+}$ solution with ionic strength $\mu = 1$ ensured by $[(Na^+, H^+)\cdot SO_4^{2-}]$ (0.33 M) or $[(Na^+, H^+)\cdot NO_3^-]$ (1 M) and initial pH adjustment ensured by $H_2SO_4$ or $HNO_3$ in thermostated polypropylene tubes at $(25 \pm 0.2)$ °C for specific times. The phases are then separated using a centrifuge separator during 10 min at a speed of 12,000 rpm. The initial and the equilibrium pH of the aqueous phase were measured with a PHN78 pHmeter (Tacussel). Aqueous solutions were analyzed for copper concentration by ICP-OES (720 ES, Varian).

The removal efficiency of copper was calculated from Eq. (1):

$$\%E = 100 \left( (C_o - C_e)/ C_o \right) \tag{1}$$

where $C_o$ (mg/L) and $C_e$ is the initial and equilibrium concentration of $Cu^{2+}$ (mg/L), respectively.

### 2.5.1 Extraction kinetics

100 mg of SBA-15 CI or SBA-16 CI and 10 mL of solution containing $Cu^{2+}$ (100 mg/L) with ionic strength $\mu = 1$ ensured by $(Na^+, H^+)$ $SO_4^{2-}$ (0.33 M) at pH 4.0, were stirred at $(25 \pm 0.2)$ °C for different times from 1 to 360 min, then separated and analyzed to assess the residual $Cu^{2+}$ concentration. Many applications, such as wastewater treatment and metal purification, need rapid extraction rate and short contact time.

### 2.5.2 Effect of pH

The effect of pH was studied within a range of 1.0–5.0. The family of HPMSP ligand was used in the liquid–liquid extraction of divalent cations [32]. Their higher acidity pKa (2.6–4.0) allows extractions at lower pH's. Particularly, they form stable extractable complexes, in acidic solutions [33, 34]. The initial metal concentration was 100 mg/L with ionic strength $\mu = 1$, while the initial pH values were adjusted by adding $H_2SO_4$ and $Na_2SO_4$ solutions or $HNO_3$ and $NaNO_3$ solutions. After 5 min of

contact at $(25 \pm 0.2)$ °C, the suspensions were separated, and analyzed for final pH (equilibrium pH) and residual $Cu^{2+}$ concentrations.

For the analysis of the extraction test, the distribution ratio, D, is denoted as:

$$D = \left[ Cu^{2+} \right]_{solid} / \left[ Cu^{2+} \right]_{aqueous} \tag{2}$$

where $[Cu^{2+}]_{solid}$ and $[Cu^{2+}]_{aqueous}$ are the metal ion concentrations in the solid phase (mol/g) and aqueous phase (mol/ml). The distribution ratio of the metal tested was calculated from the equilibrium concentrations in the solid and aqueous phase.

### 2.5.3 Extraction isotherm of $Cu^{2+}$

Extraction isotherm studies were conducted by mixing 100 mg of SBA-15 CI or SBA-16 CI with 10 mL $Cu^{2+}$ in a sulfate solution pH 4.0 with ionic strength $\mu = 1$. For the series of measurements, the initial concentration of $Cu^{2+}$ solution was controlled in the range of 100–6000 mg/L. To achieve saturated adsorption, the sample solution was shaken for 5 min at $(25 \pm 0.2)$ °C and the concentrations of the metal ions were analyzed by ICP OES after separation of the solid by centrifugation.

The capacity of removal was calculated from Eq. (3):

$$q_e = (C_o - C_e)V/m \tag{3}$$

where $q_e$ (mg/g) is the amount of copper ions extracted onto the unit amount of the solid, $C_0$ (mg/L) is the initial copper ion concentration, $C_e$ (mg/L) is the final or the equilibrium copper ion concentration, V(L) is the volume of the solution and m (g) is the solid weight in dry form.

The Freundlich and Langmuir adsorption isotherms, often used to describe the removal of solutes from a liquid phase were applied to our experimental results. Linear form of the Freundlich equation can be expressed as follows [35]:

$$\ln(q_e) = \ln(k_f) + n \ln(C_e) \tag{4}$$

where $q_e$ (mg/g) and $C_e$ (mg/L) are the equilibrium concentrations of copper in the solid and liquid phases respectively, $K_f$ and n are the Freundlich coefficients.

Linear form of the Langmuir equation can also be expressed as follows [36]:

$$C_e/ q_e = 1/ (q_m.K) + (1/q_m) C_e \tag{5}$$

where $q_e$ (mg/g) and $C_e$ (mg/L) denote the equilibrium concentrations of copper in the solid and the liquid phases respectively, $q_m$ (mg/g) is the maximum removal capacity or the amount of metal to form a complete monolayer, and K (L/g) is the Langmuir constant related to the energy of extraction [37, 38].

## 3 Results and discussion

### 3.1 Characterization
before and after the functionalization

The thermogravimetric curves (TGA) for the impregnated mesoporous silica are shown in Fig. 2. The SBA-15 C and SBA-16 C providea slight weight loss with increasing temperature, which is due to surface deshydration (at T = 80 °C) and/or deshydroxylation (at T > 250 °C) [39]. Furthermore, these are an evidence of the hydrophilic character of the calcined surface allotted to the presence of silanols groups due to an incomplete condensation upon calcination. The loss of mass for SBA16 C is lower (6 %) than for SBA15 C (8 %) attesting more hydrophilic character for SBA-15 C. The TGA curves of the SBA-15CI and SBA-16CI show two-step weight loss. The mass loss up to 150 °C is related to the physisorbed water which is 6 % for SBA-15 CI and 4 % for the SBA-16 CI, thus 2 % less than for calcined samples. This reduction is an evidence of the partial grafting of the HPMSP on the silanol groups.

The mass loss between 300 and 600 °C (22 % weight loss for the SBA-15 CI and 25 % for the SBA-16 CI) is associated to decomposition of the organic group of the HPMSP. This result is an agreement with previous results reported in the literature for other functionalized mesoporous silica [40, 41]. The lost quantity is very close to the introduced one (30 % see above). The much higher extractant loading for SBA-16 is well correlated with the less hydrophilic character for this solid as found above.

#### 3.1.1 Structure of the mesoporous materials

SAXS measurements were used to identify the hexagonal and cubic mesoporous structure of the SBA-15 C and SBA-16 C, respectively, as well as the two functionalized forms with HPMSP SBA-15 CI and SBA-16 CI (Fig. 3). The XRD patterns of the calcined SBA-15C and the impregnated SBA-15CI (Fig. 3a) exhibit one very intense peak (100) at about 0.9° and two weak peaks indexed to a hexagonal lattice as (110) and (200), which are characteristic of the hexagonal structure of SBA-15 materials [18, 42]. The highly ordered hexagonal structure is well retained after impregnation by the HPMSP ligand. The X-ray

Fig. 2 TGA analyses of (a) SBA-15 C and SBA-15 CI, (b) SBA-16 C and SBA-16 CI
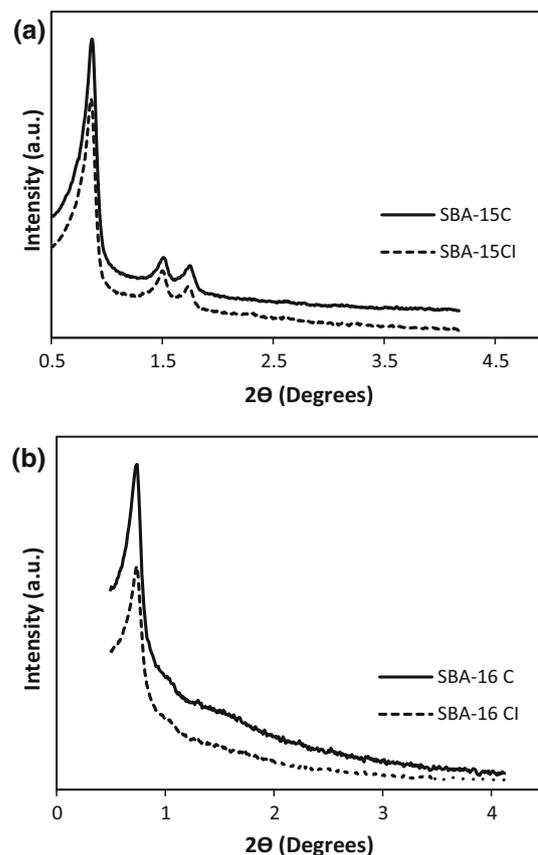
Fig. 3 Small angle XRD patterns for samples (a) SBA-15 C and SBA-15 CI; (b) SBA-16 C and SBA-16 CI
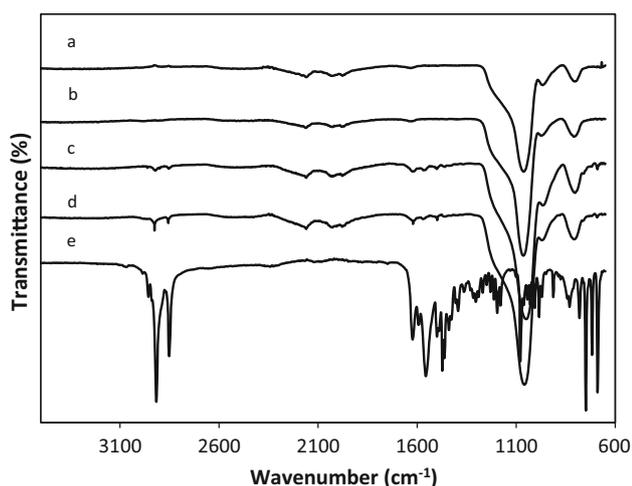
**Fig. 4** Fourier transform infrared (FT-IR) spectra of samples: *a* SBA-16 C; *b* SBA-15 C; *c* SBA-16 CI; *d* SBA-15 CI and *e* HPMSP

diffractograms of the calcined SBA-16 C and the impregnated SBA-16 CI are shown in Fig. 3b. SBA-16 C showed a strong and well resolved reflexion at $2\theta = 0.742$. This corresponds to the (110) plan, and is in good agreement with the reported patterns of the cubic (Im3m) structure of SBA-16 [43–45]. The structure of the mesoporous functionalized SBA-16 CI, is clearly remained unchanged after impregnation by HPMSP. The reduction of peak intensity is probably due to the presence of the extractant in the pores.

The FT-IR spectra of the SBA-15 and SBA-16 samples before and after HPMSP impregnation are presented in Fig. 4. The IR spectrum of SBA-15C or SBA-16 C sample is dominated by the asymmetric Si–O–Si stretching vibration at 1074 cm$^{-1}$. The band at 1676 cm$^{-1}$ is assigned to O–H bending vibration of adsorbed water molecules. The symmetric Si–O–Si stretching vibration occurs at 825 cm$^{-1}$. The band at 998 cm$^{-1}$ corresponds to Si–OH vibration generated by the presence of defect sites (silanol), which is characteristic of mesoporous silica [46]. On the other hand, the spectrum for the HPMSP exhibits the characteristic adsorption bands in the 690–2920 cm$^{-1}$ range (i.e., 1626, 1560, 2854 and 2920 cm$^{-1}$ bands can be assigned to C=O stretching of the enol form, C=C stretching vibration of the aromatic and C–H vibration of the alkyl chain, respectively) [47, 48]. These bands also appear in the SBA-15 CI and SBA-16 CI samples, which imply that HPMSP has been incorporated in the structure of the mesoporous silica.

### 3.1.2 Specific surface area and porosity

Compared to the XRD characterization, nitrogen physisorption provides the bulk-averaged information of the mesoporous materials. In this study, nitrogen physisorption

was conducted to complete XRD measurement, determining the porous structure, surface area, pore size and volume of the SBA. For the SBA-15 C and SBA-15 CI (Fig. 5a), the N$_2$ isotherms are of type IV and show a clear H1 type hysteresis loop suggesting that those materials have very regular mesoporous channels. On the other hand, the SBA-16 C presents a type IV nitrogen adsorption isotherm with a pronounced hysteresis loop characteristics for cage-like materials with interconnected uniform mesopores. Similarly to the parent material, SBA-16 CI (Fig. 5b) also shows a type IV isotherm with an H2 hysteresis loop, indicating that the SBA-16 impregnated still maintains a good mesoporous cage-like structure.

The specific BET surface area, pore volume and average pore diameter calculated from N$_2$ adsorption isotherms are summarized in Table 1. All the calculate values are in good agreement with the results reported elsewhere [49, 50]. All the pore structure parameters of SBA-15 CI and SBA-16 CI decrease obviously compared to parent SBA-15 C and
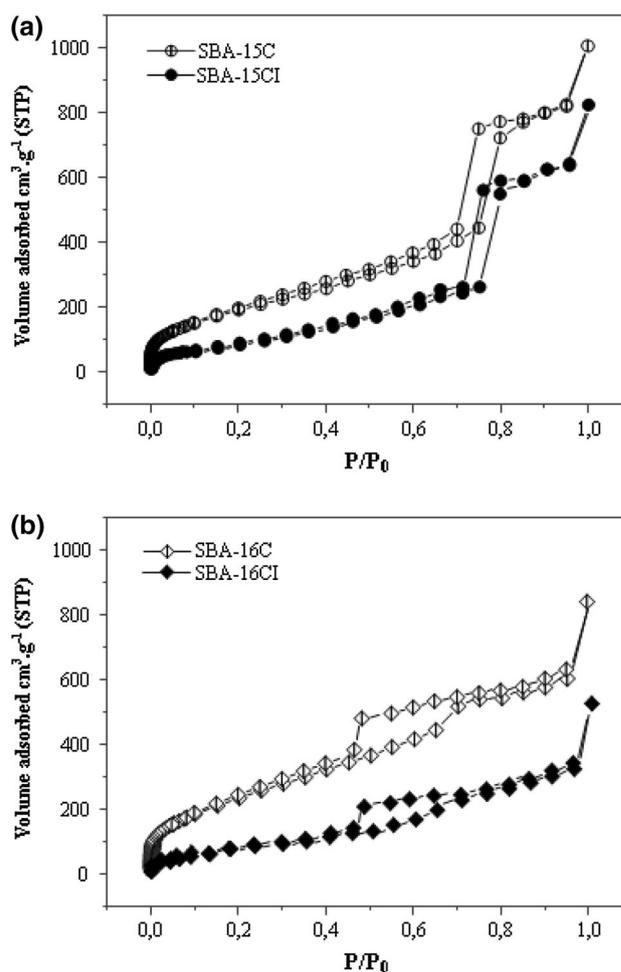


**Fig. 5** N$_2$ adsorption–desorption isotherms for (**a**) SBA-15C and SBA-15CI, (**b**) SBA-16C and SBA-16CI

**Table 1** Characteristics of SBA-15C, SBA-15CI, SBA-16C and SBA-16CI samples

| Sample | Surface area(BET) ($m^2/g$) | Pore size for desorption branch (nm) | Pore size for adsorption branch (nm) | Volume pore ($cm^3/g$) |
|---|---|---|---|---|
| SBA-15C | 897 | 6.6 | 9.7 | 0.69 |
| SBA-15CI | 348 | 5.8 | 8.9 | 0.59 |
| SBA-16C | 708 | 3.63 | 6.32 | 0.79 |
| SBA-16CI | 197 | 3.43 | 6.1 | 0.39 |
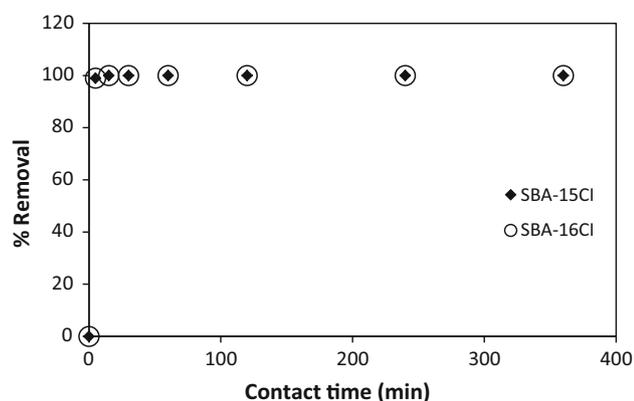


**Fig. 6** Influence of the contact time on the copper removal by SBA-15CI and SBA-16CI (Temperature $(25 \pm 0.2)$ °C, $pH_0 = 4$, $[(Na,H)SO_4] = 0.33$ M and $[Cu^{2+}]_0 = 1.57$ mmol/L)

SBA-16 C. In the case of the cubic structure SBA-16 these structure parameters decrease more sensibly. These results further support the statement that HPMSP ligand has been incorporated into the channels of the SBA-16 C, and hence reduce the pore volume of the parent materials [51].

The results of the textural characterization are well correlated with the TGA analysis and the SAXS measurements and attest that the organic extractant is not only loaded inside the pores but also is partially grafted to the pore walls.

## 3.2 Copper extraction

### 3.2.1 Kinetic study of copper extraction

Figure 6 shows the adsorption variation of $Cu^{2+}$ by impregnated mesoporous silica SBA-15 CI and SBA-16 CI as a function of contact time, copper can be totally removed (99.99 %) by the two functionalized mesoporous silicas after less than 5 min.

The extraction kinetics is very fast as attested by the immediate green coloration of the solution of Cu (II) colorless after the contact between functionalized mesoporous silica. At the best of our knowledge, all the already tested adsorbent and extractant [34, 52] have never reached a similar fast and efficient capacity of copper removal in few minutes. For example, the (Doped HPMSP-MCM-41) removes the totality of copper but in a contact time of 60 min. However, functionalized materials (SBA-15CI and SBA-16CI) reach the same efficiency in only 5 min which is very fast. Table 2 shows a comparison of the efficiency removal and time contact of various adsorbents.

### 3.2.2 Effect of pH

The effect of the equilibrium pH value on the $Cu^{2+}$ adsorption in a sulfate medium with SBA-15 and SBA-16 are given in Fig. 7. The results show that copper is not significantly extracted by SBA samples ever calcined or not calcined. For the impregnated SBA samples, we clearly noticed a decrease of the pH during the extraction (initial pH > equilibrium pH). As a result, the extraction process is likely an ion exchange between $Cu^{2+}$ in aqueous phase and $H^+$ protons of HPMSP in the solid phase, i.e. the same process obtained in the liquid–liquid extraction of copper by HPMSP [34, 57], and the solid–liquid extraction of copper using functionalized MCM-41 [17, 56]. The $Cu^{2+}$ removal efficiency increases as the solution pH increases from 1 to 3 and then it remains constant with further pH increase. Copper ion can be totally removed (99.99 %)

**Table 2** Copper removal results on different adsorbents

| Adsorbent | $[Cu^{2+}]_0$ (mg/L) | Temperature (°C) | Time contact (min) | % Removal | References |
|---|---|---|---|---|---|
| Grafted SBA-15 with trimethoxysilylpropyle dithyenetriamine | 100 | 25 | 1440 | 59 | [53] |
| SBA-15 functionalized with 3-aminopropyltri-methoxy-silane | 80 | 60 | 120 | 36 | [54] |
| MDA-magMCM-48 | 80 | 25 | 90 | 83 | [55] |
| Doped HPMSP-MCM-41 | 100 | 25 | 60 | 100 | [56] |
| Doped DEHPA-MCM-41 | 100 | 25 | 60 | 20 | [56] |
| SBA-15CI | 100 | 25 | 5 | 99.99 | This study |
| SBA-16CI | 100 | 25 | 5 | 99.99 | This study |

**Fig. 9** Extraction isotherms of $Cu^{2+}$ on the SBA-15 CI and SBA-16 CI (Temperature $(25 \pm 0.2)$ °C, $t = 5$ min, $pH_0 = 4$ and $[(Na,H)SO_4] = 0.33$ M)

extraction for $Cu^{2+}$ onto the impregnated mesoporous SBA-15 CI or SBA-16 CI coefficient, Keq is defined as:

$$Keq = [CuL_2]_{silica}[H^+]^2 / [Cu^{2+}] [HL]^2_{silica} \qquad (6)$$

Equation (2) was used to calculate and plot of log D for copper versus equilibrium (Fig. 8). We obtain for the two supports a straight line of slope respectively 1.83 and 1.64 which indicates the release of $2H^+$ leading to the extraction of copper as $CuL_2$ [34].

### 3.2.3 Extraction capacity of the SBA-15 CI and SBA-16 CI

The plot of $Cu^{2+}$ removed by SBA-15 CI and SBA-16 CI in a sulfate medium versus the initial metal concentration is shown in Fig. 9. The experience is repeated for each initial concentration of: 100, 300, 600, 800, 1500, 3500 and 6000 ppm. With the increase of the initial metal concentration, the amount of $Cu^{2+}$ removal by these materials increased. At low initial metal ion concentrations, the ratio



**Fig. 7** Removal of $Cu^{2+}$ by (**a**) SBA-15 and (**b**) SBA-16 as a function of pH (Temperature $25 \pm 0.2$ °C, $t = 5$ min, $[(Na,H)SO_4] = 0.33$ M and $[Cu^{2+}]_0 = 1.57$ mmol/L)

when the pH is over 3. At pH < 1, only 10 % of $Cu^{2+}$ was adsorbed with SBA-15CI while the $Cu^{2+}$ adsorption rate was 50 % for SBA-16CI.

The reaction equation for the extraction of divalent metal ions onto SBA-15CI and SBA-16CI can be described as follows:

$$Cu^{2+} + 2 [HL]_{silica} \Leftrightarrow [CuL_2]_{silica} + 2H^+$$

where $[HL]_{silica}$ the ligand HPMSP into the mesoporous materials SBA-15 C or SBA-16 C. The equilibrium

**Fig. 8** Plot of log D versus equilibrium pH with (**a**) SBA-16CI and (**b**) SBA-15CI (Temperature $(25 \pm 0.2)$ °C, $t = 5$ min, $[(Na,H)SO_4] = 0.33$ M and $[Cu^{2+}]_0 = 1.57$ mmol/L)

**Table 3** Extraction isotherm constants for $Cu^{2+}$ on SBA-15 CI and SBA-16 CI

| Adsorption isotherm | Parameter | SBA-15 CI | | SBA-16 CI | |
|---|---|---|---|---|---|
| | | Value of parameter | $R^2$ | Value of parameter | $R^2$ |
| Langmuir | K(L/g) | 6.94 | 0.9982 | 20.86 | 0.9998 |
| | $q_m$ (mg/g) | 22.72 | | 25.83 | |
| Freundlich | $K_f$ (L/g) | 5.19 | 0.8815 | 16.56 | 0.8403 |
| | 1/n | 0.17 | | 0.11 | |
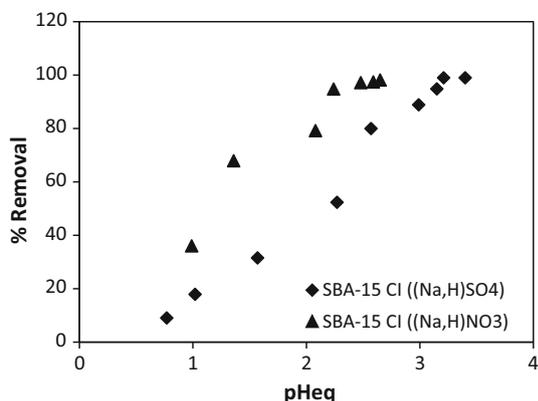


**Fig. 10** Removal of $Cu^{2+}$ by SBA-15 CI as a function of pH (Temperature $(25 \pm 0.2)$ °C, t = 5 min, $[(Na,H)NO_3] = 1$ M, $[(Na,H)SO_4] = 0.33$ M and $[Cu^{2+}]_0 = 1.57$ mol/L)
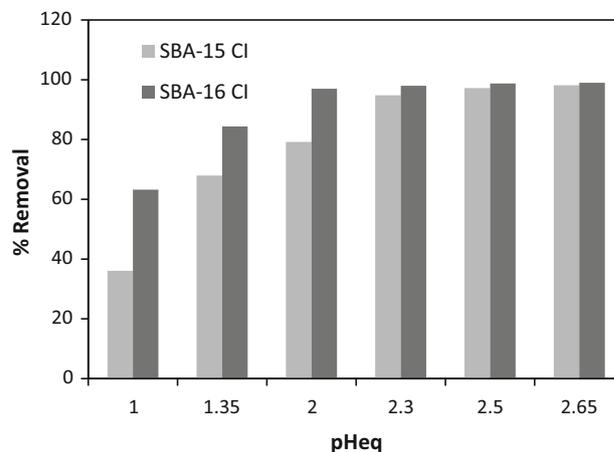


**Fig. 12** % Removal of copper versus equilibrium pH (Temperature $(25 \pm 0.2)$ °C, t = 5 min, $[(Na,H)NO_3] = 1$ M and $[Cu^{2+}]_0 = 1.57$ mmol/L)
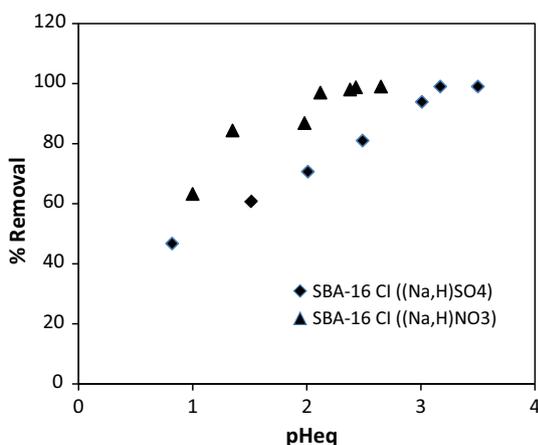


**Fig. 11** Removal of $Cu^{2+}$ by SBA-16 CI as a function of pH (Temperature $(25 \pm 0.2)$ °C, t = 5 min, $[(Na,H)NO_3] = 1$ M, $[(Na,H)SO_4] = 0.33$ M and $[Cu^{2+}]_0 = 1.57$ mmol/L)

of $Cu^{2+}$ to the number of available adsorption sites or ions exchange site is small and consequently the adsorption is 99.99 % and independent of the initial concentration. At higher metal concentration, a unit mass of the solid is exposed to a large number of metal ions and progressively, higher number of metal ions is taken up with the gradual filling up of the appropriate binding sites. This gives an increase in the amount of $Cu^{2+}$ removed while the percent extraction decreased from 99.99 to 36 %.

Langmuir and Freundlich equations (Eqs. 5 and 6) were used to analyze the experimental data (Table 3)

The Langmuir model is basically developed to describe the adsorption processes where no interaction between sorbate species occurs on sites having the same extraction energies independently of surface coverage. Maximum extraction capacity represents the monolayer coverage of solid with metal. It is well known that Freundlich isotherm applies to non specific extraction and heterogeneous sites on solid surfaces, so the isotherm is valid for weak Van Der Waals' type adsorption as well as for strong chemisorptions [58]. In this work, it is observed that the extraction data fits better the Langmuir isotherm equation. Thus, the extraction behavior of our materials for $Cu^{2+}$ most likely belongs to monolayer adsorption. This indicates that the monolayer reaction of $Cu^{2+}$ on both the SBA-15 CI and SBA-16 CI was predominant [59] and SBA-16 CI with a greater capacity (25.8 mg/g) is more efficient than SBA-15 CI (22.7 mg/g). This last result is well correlated to the much higher extractant loading of SBA-16 as compared with SBA-15. One can deduce that the geometrical organization of the channels (hexagonal or cubic) has no effect on the extraction capacity.

### 3.2.4 Effect of the counter-ion

The effect of the copper counter-ion on the $Cu^{2+}$ extraction at different values of pH equilibrium was also studied. The initial metal concentration was 100 mg/L and the initial pH values were adjusted by adding $HNO_3$ solution, the result is shown in Figs. 10 and 11. The presence of $NO_3^-$ has a clear effect on the corresponding $Cu^{2+}$ adsorption capacity particularly when the pH is <3. $SO_4^{2-}$ species can react with $Cu^{2+}$ to form stable complex at low pH (<3) and thus influence the copper removal as it has been observed by Xue and Li [60] in the study of the counter-ions effect on the functionalized SBA-16 copper adsorption.

### 3.2.5 Effectiveness comparison

According to Fig. 12, SBA-16 CI is leading always to better copper removal compared to SBA-15 CI in acidic media pH $\leq$ 2. There is a clear difference between the two modified materials SBA-15 CI and SBA-16 CI (reaching 40 %). The tridimensional structure of SBA-16 allowing facile diffusion of the organic group of ligand HPMSP into the mesopores is probably responsible of this difference which can be already explained by the preceding results of the thermogravimetric (TGA). Umetani et al. [61] demonstrate that each mesopore in the body-centered cubic array (SBA-16) is connected to eight neighbors. This provides more favorable mass transfer compared to the uni-directional pore system of hexagonal mesoporous materials such as SBA-15 [62].

## 4 Conclusion

Impregnation of ligand HPMSP on SBA-15 and SBA-16 will not change the mesoporous structure and removal of $Cu^{2+}$ by these functionalized materials was investigated as a function of equilibration time, pH equilibrium, the presence of the counter-ion and initial metal concentration. The extraction kinetics is very fast as attested by the immediate green coloration of the materials. The removel of $Cu^{2+}$ increases as pH value is raised from 1 to 5 and copper ion can be totally removed (99.99 %) for pH values over 3.2. The nature of the counter-ion ($NO_3^-$ or $SO_4^{2-}$) affects the copper extraction particularly at pH < 3. The $SO_4^{2-}$ entities in solution can compete with impregnated HMPSP ligand for the complexation of $Cu^{2+}$, decreasing the extraction on the solids. Also at pH < 3, removal efficiency is better with SBA-16 CI than SBA-15 CI. The extraction of $Cu^{2+}$ ions shows best fit to the Langmuir isotherm equation. This indicates the predominance of monolayer reaction of $Cu^{2+}$ on the SBA-15 CI or SBA-16 CI. The maximum extraction amount for SBA-15 CI and SBA-16 CI is 22.7 and 25.8 mg/g respectively. The impregnated materials SBA-15 CI and SBA-16 CI might act as performing cleanup systems need rapid extraction for acid solutions contaminated by heavy metals such as copper.

## References

1. C. Quintelas, Z. Rocha, B. Silva, B. Fonseca, H. Figueiredo, T. Tavares, Chem. Eng. J. **149**, 319 (2009)
2. Y.K. Sun, G.M. Zhou, X.M. Xiong, X.H. Guan, L.N. Li, H.L. Bao, Water Res. **47**, 4340 (2013)
3. H. Chen, X.L. Sheng, Y.Z. Wen, L.J. Zhang, H.L. Bao, L.N. Li, W.P. Liu, Aquat. Toxicol. **140**, 407 (2013)
4. Y. Zhang, X.Y. Cai, X.M. Lang, X.L. Qiao, X.H. Li, J.W. Chen, Environ. Pollut. **166**, 48 (2012)
5. L. Agouborde, R. Navia, J. Hazard. Mater. **167**, 536 (2009)
6. S. Chakravarty, S. Pimple, H.T. Chaturvedi, S. Singh, K.K. Gupta, J. Hazard. Mater. **159**, 396 (2008)
7. Y. Jiang, H. Pang, B. Liao, J. Hazard. Mater. **164**, 1 (2009)
8. D.J. Ennigrou, M.B.S. Ali, M. Dhahbi, Desalination **343**, 82 (2014)
9. S. Anirudhan, S. Rijith, Colloids Surf. A Physicochem. Eng. Asp. **351**, 52 (2009)
10. J. González-Mu¡noz, M.A. Rodríguez, S. Luque, J.R. Àlvarez, Desalination **200**, 742 (2006)
11. M. Baker, A.M. Massadeh, H.A. Younes, Environ. Monit. Assess. **157**, 319 (2009)
12. H.K. Shon, S. Vigneswaran, M.H. Zareie, R. Ben Aim, E. Lee, J. Lee, J. Cho, S. Kim, Desalination **236**, 282 (2009)
13. L. Cortina, N. Miralles, M. Aguilar, A. Warshawsky, React. Funct. Polym. **27**, 61 (1995)
14. J.L. Cortina, N. Miralles, M. Aguilar, A.M. Sastre, Hydrometallurgy **40**, 195 (1996)
15. A.G. Strikovsky, K. Jerabek, J.L. Cortina, A.M. Sastre, A. Warshawsky, React. Funct. Polym. **28**, 149 (1996)
16. S. Chegrouche, A. Mellah, S. Telmoune, Water Res. **31**, 1733 (1997)
17. H. Miloudi, A. Boos, D. Bouazza, T. Ali-Dahmane, A. Tayeb, G. Goetz-Grandmont, A. Bengueddach, Mater. Res. Bull. **42**, 769 (2007)
18. D. Zhao, Q. Huo, J. Feng, F. Chmelka, G.D. Stucky, J. Am. Chem. Soc. **120**, 6024 (1998)
19. T.W. Kim, R. Ryoo, M. Kruk, K.P. Gierszal, M. Jaroniec, S. Kamiya, O. Terasaki, J. Phys. Chem. B **108**, 11480 (2004)
20. S. Duan, X. Zhang, S. Xu, C.L. Zhou, Electrochim. Acta **88**, 885 (2013)
21. N. Bouazizi, R. Ouargli, S. Nousir, R. Ben Slama, A. Azzouz, J. Phys. Chem. Solids **77**, 172 (2015)
22. Q. Huo, D.I. Margolese, U. Ciesla, D.G. Demuth, P. Feng, T.E. Gier, P. Sieger, A. Firouzi, B.F. Chmelka, F. Schüth, G.D. Stucky, Chem. Mater. **6**, 1176 (1994)
23. Q. Huo, D.I. Margolese, G.D. Stucky, Chem. Mater. **8**, 1147 (1996)
24. P. Van Der Voort, P.I. Ravikovitch, K.P. De Jong, M. Benjelloun, E. Van Bavel, A.H. Janssen, A.V. Neimark, B.M. Weckhuysen, E.F. Vansant, J. Phys. Chem. B **106**, 5873 (2002)
25. P. Kipkemboi, A. Fogden, V. Alfredsson, K. Flodström, Langmuir **17**, 5398 (2001)
26. F. Kleitz, T.W. Kim, R. Ryoo, Bull. Korean Chem. Soc. **26**, 1653 (2005)

27. A.B. Fuertes, Mater. Lett. **58**, 1494 (2004)
28. C. Lesaint, F. Frébault, C. Delacôte, B. Lebeau, C. Marichal, A. Walcarius, J. Patarin, Surf. Sci. Catal. **156**, 925 (2005)
29. S.C. Han, E. Sujandi, S.E. Park, Bull. Korean Chem. Soc. **26**, 1381 (2005)
30. T.W. Kim, R. Ryoo, K.P. Gierszal, M. Jaroniec, L.A. Solovyov, Y. Sakamoto, O. Terasaki, J. Mater. Chem. **15**, 1560 (2005)
31. B.S. Jensen, Acta Chem. Scand. **13**, 1668 (1959)
32. G.J. Sigit, G.J. Goetz-Grandmont, J.P. Brunette, Monatsh. Chem. **129**, 787 (1998)
33. E. Bou-Maroun, G.J. Goetz-Grandmont, A. Boos, Sep. Sci. Technol. **42**, 1913 (2007)
34. E. Bou-Maroun, G.J. Goetz-Grandmont, A. Boos, Colloid Surf. A. **287**, 1 (2006)
35. H. Freundlich, H.S. Hatfield, *Colloid and Capillary Chemistry* (Methuen & Co. Ltd., London, 1926), p. 993
36. I. Langmuir, J. Am. Chem. Soc. **38**, 2221 (1916)
37. K.G. Bhattacharyya, S.S. Guptaa, J. Colloid Interface Sci. **310**, 411 (2007)
38. I. Langmuir, J. Am. Chem. Soc. **40**, 1361 (1918)
39. Z. Luan, J.A. Fournier, J.B. Wooten, D.E. Miser, Microporous Mesoporous Mater. **83**, 150 (2005)
40. L. Bois, L. Bonhommé, A.A. Ribes, B. Pais, G. Raffin, F. Tessier, Colloids Surf. A Physicochem. Eng. Asp. **221**, 221 (2003)
41. D.P. Quintanilla, A. Sanchez, I.D. Hierro, M. Fajardo, I. Sierra, J. Hazard. Mater. **166**, 1449 (2009)
42. D. Zhao, J. Feng, Q. Huo, N. Melosh, G.H. Fredickson, B.F. Chmelka, G.D. Stucky, Science **279**, 548 (1998)
43. J.J.S. Wesley, M. Myrjam, M. Steven, T. Ivo, V.T. Gustaaf, C. Pegie, F.V. Etienne, Microporous Mesoporous Mater. **93**, 119 (2006)
44. J. Aburto, M. Ayala, I. Bustos-Jaimes, C. Montiel, E. Terres, J.M. Dominguez, E. Torres, Microporous Mesoporous Mater. **83**, 193 (2005)
45. J.C. Amezcua, L. Lizama, C. Salcedo, I. Puente, J.M. Dominguez, T. Klimova, Catal. Today **107**, 578 (2005)
46. M.D. Alba, Z.H. Luan, J. Klinowski, J. Phys. Chem. **100**, 2178 (1996)
47. T. Ueda, Y. Akama, Chem. Phys. Lett. **222**, 559 (1994)
48. E.C. Okafor, Spectrochim. Acta Part A Mol. Spectrosc. **40**, 397 (1984)
49. Y. Chen, H. Lim, Q. Tang, Y. Gao, T. Sun, Q. Yan, Y. Yang, Appl. Catal. A **380**, 55 (2010)
50. F. Kleitz, T.W. Kim, R. Ryoo, Langmuir **22**, 440 (2006)
51. Q. Cheng, V. Pavlinek, A. Lengalova, C. Li, Y. He, P. Saha, Microporous Mesoporous Mater. **93**, 263 (2006)
52. K.A. Northcotta, K. Miyakawab, S. Oshimac, Y. Komatsub, J.M. Pereraa, G.W. Stevensa, Chem. Eng. J. **157**, 25 (2010)
53. J. Aguado, J.M. Arsuaga, A. Arencibia, M. Lindo, V. Gascón, J. Hazard. Mater. **163**, 213 (2009)
54. E. Da'na, A. Sayari, Desalination **285**, 62 (2012)
55. M. Anbia, K. Kargosha, S. Khoshbooei, Chem. Eng. Res. Des. **93**, 779 (2015)
56. H. Miloudi, A. Tayeb, A. Boos, Z. Mehyou, G.J. Goetz-Grandmont, A. Bengueddach, Arab. J. Chem. (2013). doi:10.1016/j.arabjc.2013.06.023
57. K. Torkestani, O. Blinova, J. Arichi, G.J. Goetz-Grandmont, J.P. Brunette, Solv. Extr. Ion Exch. **14**, 1037 (1996)
58. N.C.D. Rocha, R.C.D. Campos, A.M. Rossi, E.L. Moreira, A.D.F. Barbosa, G.T. Moure, Environ. Sci. Technol. **36**, 1630 (2002)
59. R. Zhu, R. Yu, J. Yao, D. Mao, C. Xing, D. Wang, Catal. Today **139**, 94 (2008)
60. X. Xue, F. Li, Microporous Mesoporous Mater. **116**, 116 (2008)
61. S. Umetani, Q.T.H. Le, M. Matsui, Anal. Sci. **13**, 103 (1997)
62. Y. Sakamoto, M. Kaneda, O. Terasaki, D.Y. Zhao, J.M. Kim, G. Stucky, H.J. Shin, R. Ryoo, Nature **408**, 449 (2000)